

# Self-dual solitons in a $CPT$ -odd and Lorentz-violating gauged $O(3)$ sigma model

R. Casana,<sup>\*</sup> C. F. Farias,<sup>†</sup> M. M. Ferreira, Jr.,<sup>‡</sup> and G. Lazar<sup>§</sup>

<sup>1</sup>*Departamento de Física, Universidade Federal do Maranhão, 65080-805, São Luís, Maranhão, Brazil.*

We have performed a complete study of self-dual configurations in a  $CPT$ -odd and Lorentz-violating gauged  $O(3)$  nonlinear sigma model. We have consistently implemented the Bogomol'nyi-Prasad-Sommerfield (BPS) formalism and obtained the correspondent differential first-order equations describing electrically charged self-dual configurations. The total energy and magnetic flux of the vortices, besides being proportional to the winding number, also depend explicitly on the Lorentz-violating coefficients belonging to the sigma sector. The total electrical charge is proportional to the magnetic flux such as it occurs in Chern-Simons models. The Lorentz violation in the sigma sector allows one to interpolate between Lorentz-violating versions of some sigma models: the gauged  $O(3)$  sigma model and the Maxwell-Chern-Simons  $O(3)$  sigma model. The Lorentz violation enhances the amplitude of the magnetic field and BPS energy density near the origin, augmenting the deviation in relation to the solutions deprived of Lorentz violation.

PACS numbers: 11.10.Lm, 11.27.+d, 12.60.-i, 74.25.Ha

## I. INTRODUCTION

In the early 1960s Gell-Mann and Levy [1], based on the works of Schwinger [2] and Polkinghorne [3], constructed a renormalizable field theory for the new scalar mesons  $\sigma$  with null isotopic spin, being this theory called the sigma model. These authors considered the possibility of modifying the sigma model by supposing it as a composite of the pion field rather than an elementary one describing a new particle. This was the arising of the nonlinear sigma model (NL $\sigma$ M), which featured an  $O(4)$  symmetry initially. Later, the model was endowed with an  $O(3)$  symmetry, the  $O(3)$  NL $\sigma$ M [4], started to gain special attention and was widely applied to study different aspects of field theory and condensed matter physics [5]. The  $O(3)$  NL $\sigma$ M is also interesting because it provides topological solitons whose equations are exactly integrable in the Bogomol'nyi-Prasad-Sommerfield (BPS) limit [6]. The solutions of these BPS equations describe a map from a spherical surface that represents the two-dimensional physical space to a spherical surface in the internal field space, being classified according to the second homotopy group  $\Pi_2(S_2) = \mathbb{Z}$ . This model, however, has a serious inconvenience because the solutions are scale invariant preventing one from describing localized particles [7]. A way for breaking the scale invariance is gauging the  $U(1)$  subgroup and providing a spontaneous symmetry breaking potential. Such mechanism was suggested in Ref. [8], where a Maxwell term controlling the gauge field dynamics was introduced, so that topological solitons with arbitrary magnetic flux were engendered. A similar mechanism was implemented in Ref. [9] with the Abelian Chern-Simons in the gauge sector,

implying topological and nontopological solitons. These two approaches produce topological solitons which are infinitely degenerate in a given topological sector. Such degenerescence was circumvented in Refs. [10, 11] by means of the introduction of a self-interacting potential possessing a symmetry breaking minima. This potential induces a new topology in which the infinite circle of physical space is mapped on the equatorial circle of the internal space so that the solitons are now classified by the first homotopy group  $\Pi_1(S_1) = \mathbb{Z}$ . The  $O(3)$  sigma model has also been analyzed with the gauge field dynamics ruled by both the Maxwell and Chern-Simons terms [12, 13]. In the same context, but with a nonminimally coupled gauge field, charged BPS soliton solutions were found [14], revealing a magnetic flux quantized only for topological solitons.

Investigation of topological defects in different theoretical contexts has been a sensitive matter in the latest years. Among the new frameworks are the  $CPT$ - and Lorentz-violating (LV) field theories. The violation of the  $CPT$  and Lorentz symmetries is a theoretical possibility that has been extensively investigated since 1996, mainly in the framework of the standard model extension (SME) [15, 16], with several repercussions [17–19]. In LV theories, the formation of defects was considered in many situations, for example, in solitons generated by scalar fields [20], general defects modified by tensor fields [21], Abelian monopoles [22] and oscillons [23]. BPS vortex solutions in Abelian Higgs models including Lorentz-violating terms have been extensively examined in Refs. [24–29]. The effects of  $CPT$ -even LV terms on the topological BPS configurations of the gauged  $O(3)$  sigma model were recently studied in Ref. [30], with the achievement of a generalization of the results of the gauged  $O(3)$  sigma models studied in Refs. [10, 11].

In this manuscript, we analyze the self-dual structure of the gauged  $O(3)$  sigma model provided with  $CPT$ -odd and  $CPT$ -even Lorentz-violating terms. More specifically, we have modified the dynamics of the Maxwell sector with the  $CPT$ -odd Carroll-Field-Jackiw term [31],

<sup>\*</sup>Electronic address: [rodolfo.casana@gmail.com](mailto:rodolfo.casana@gmail.com)

<sup>†</sup>Electronic address: [cfarias@gmail.com](mailto:cfarias@gmail.com)

<sup>‡</sup>Electronic address: [manojr.ufma@gmail.com](mailto:manojr.ufma@gmail.com)

<sup>§</sup>Electronic address: [gzsabito@gmail.com](mailto:gzsabito@gmail.com)

whereas a *CPT*-even LV term was included in the  $O(3)$  sigma sector. The suitable projection of this Lagrangian in (1+2)-dimensions yields a model similar to Maxwell-Chern-Simons gauged  $O(3)$  sigma model (MCS $\sigma$ M) including LV terms in the scalar sigma sector. Next, we have implemented the BPS formalism and written the self-dual equations describing the self-dual configurations of this *CPT*-odd and LV model. To assess the repercussion of the LV terms on the self-dual configurations of the gauged  $O(3)$  sigma model, we have found the rotationally symmetric vortex solutions. These solutions possess finite energy proportional to the topological charge. The LV model provides some interesting limits connecting different versions of the gauge  $O(3)$  sigma model. The profiles are obtained numerically and compared with the ones in the total absence of Lorentz-violation in order to highlight the LV effects. Finally, we present our final remarks and conclusions.

## II. A *CPT*-ODD AND LORENTZ-VIOLATING GAUGED $O(3)$ SIGMA MODEL

The (1+2)-dimensional gauged  $O(3)$  sigma model (M $\sigma$ M) introduced in Refs. [8, 10, 11] is defined by the following Lagrangian density

$$\mathcal{L}_{M\sigma M} = -\frac{1}{4}F_{\mu\nu}F^{\mu\nu} + \frac{1}{2}D^\mu\vec{\phi}\cdot D_\mu\vec{\phi} - U(\vec{\phi}), \quad (1)$$

where  $A_\mu$  is the gauge field and  $F_{\mu\nu} = \partial_\mu A_\nu - \partial_\nu A_\mu$  is the Abelian strength tensor field. The field  $\vec{\phi} = (\phi_1, \phi_2, \phi_3)$  is a triplet of real scalar fields constituting a vector in the internal space, with fixed norm  $\vec{\phi}\cdot\vec{\phi} = 1$ , describing the  $O(3)$  NL $\sigma$ M. The coupling between the Abelian gauge and sigma field is ruled by the minimal covariant derivative

$$D_\mu\vec{\phi} = \partial_\mu\vec{\phi} - A_\mu\hat{n}_3 \times \vec{\phi}, \quad (2)$$

with  $\hat{n}_3$  being a unitary vector along the 3-direction in the internal scalar field space, while  $U(\vec{\phi})$  is the self-interacting potential.

In order to include Lorentz violation, we consider the (1+3)-dimensional version of model (1) supplementing it with the *CPT*-odd Carroll-Field-Jackiw (CFJ) term in the gauge sector and a *CPT*-even term in the sigma field sector. This way, the *CPT*-odd Lagrangian density describing the proposed Lorentz-violating sigma model is

$$\begin{aligned} \mathcal{L} = & -\frac{1}{4}F_{\mu\nu}F^{\mu\nu} - \frac{1}{4}\epsilon^{\mu\nu\rho\sigma}(k_{AF})_\mu A_\nu F_{\rho\sigma} \\ & + \frac{1}{2}D^\mu\vec{\phi}\cdot D_\mu\vec{\phi} + \frac{1}{2}(k_{\phi\phi})^{\mu\nu} D_\mu\vec{\phi}\cdot D_\nu\vec{\phi} - U. \end{aligned} \quad (3)$$

The four-vector  $(k_{AF})_\alpha$  is the CFJ background with mass dimension +1. The dimensionless tensor  $(k_{\phi\phi})^{\mu\nu}$  is real and symmetric, containing the LV and *CPT*-even parameters in the sigma sector. The potential  $U$  describes

some convenient interaction producing self-dual configurations, still to be determined.

From the Lagrangian density (3), the equation of motion for the gauge field reads

$$\partial_\nu F^{\nu\mu} + \frac{1}{2}\epsilon^{\mu\alpha\rho\sigma}(k_{AF})_\alpha F_{\rho\sigma} = j^\mu, \quad (4)$$

where the conserved current density in this LV framework,

$$j^\mu = [g^{\mu\nu} + (k_{\phi\phi})^{\mu\nu}]\hat{n}_3 \cdot (\vec{\phi} \times D_\nu\vec{\phi}), \quad (5)$$

is the counterpart of the one in absence of Lorentz violation,  $j^\mu = \hat{n}_3 \cdot (\vec{\phi} \times D^\mu\vec{\phi})$ , displayed in Ref. [11]. The equation of motion for the sigma field is

$$\begin{aligned} [g^{\mu\nu} + (k_{\phi\phi})^{\mu\nu}]D_\mu D_\nu\vec{\phi} = & \left(\vec{\phi}\cdot\frac{\partial U}{\partial\vec{\phi}}\right)\vec{\phi} - \frac{\partial U}{\partial\vec{\phi}} \\ & + [g^{\mu\nu} + (k_{\phi\phi})^{\mu\nu}]\left(\vec{\phi}\cdot D_\mu D_\nu\vec{\phi}\right)\vec{\phi}. \end{aligned} \quad (6)$$

From now on we are interested in the topological self-dual configurations arising from the (1+2)-dimensional version of the model (3). For such a purpose to be fulfilled, we implement a projection procedure doing  $\partial_3\vec{\phi} = 0$ ,  $A_3 = 0$ ,  $\partial_3 A_\mu = 0$  ( $\mu = 0, 1, 2$ ). Besides, it is necessary to impose  $(k_{\phi\phi})_{0i} = 0$ . In this way, from (4), the planar stationary Gauss law is

$$\partial_j\partial_j A_0 - (k_{AF})_3 B = [1 + (k_{\phi\phi})_{00}][(\phi_1)^2 + (\phi_2)^2]A_0, \quad (7)$$

and the planar stationary Ampere law reads

$$\epsilon_{ij}\partial_j B - (k_{AF})_3\epsilon_{ij}\partial_j A_0 = -[\delta_{ij} - (k_{\phi\phi})_{ij}]\hat{n}_3 \cdot (\vec{\phi} \times D_j\vec{\phi}), \quad (8)$$

where  $B \equiv B_3 = F_{12}$  defines the magnitude of the magnetic field along the  $z$ -axis and Latin indexes run over  $i, j = 1, 2$ . Here, we point out that the magnetic field  $B = F_{12}$  is effectively a planar or "scalar" version of the 3D-magnetic field  $B_k = \epsilon_{kmn}F_{mn}/2$ . Both equations clearly show that the LV coefficient  $(k_{AF})_3$  is responsible for the coupling between electric and magnetic sectors, allowing, in principle, the occurrence of electrically charged configurations. The  $(k_{AF})_3$  coefficient in both the Gauss and Ampere laws plays a similar role of the Chern-Simons mass in the (1 + 2)-dimensional Maxwell-Chern-Simons gauged  $O(3)$  sigma model (MCS $\sigma$ M) [12, 13], defined by

$$\begin{aligned} \mathcal{L}_{MCS\sigma M} = & -\frac{1}{4}F_{\alpha\beta}F^{\alpha\beta} - \frac{1}{4}\kappa\epsilon^{\beta\rho\sigma}A_\beta F_{\rho\sigma} \\ & + \frac{1}{2}D^\alpha\vec{\phi}\cdot D_\alpha\vec{\phi} + \frac{1}{2}\partial_\mu\Psi\partial^\mu\Psi \\ & - \frac{1}{2}[(\phi_1)^2 + (\phi_2)^2]\Psi^2 - U(|\phi|, \Psi), \end{aligned} \quad (9)$$

where  $\kappa$  is the Chern-Simons mass,  $U(|\phi|, \Psi)$  is the self-dual potential and  $\Psi$  is a neutral field. The introduction

of this neutral scalar field is a well established procedure for a consistent description of self-dual configurations, and it was first reported in the context of Maxwell-Chern-Simons-Higgs models [32] based in supersymmetric arguments. It was also successfully implemented in other subsequent extensions [33], including to describe charged topological configurations in Lorentz-violating models [25, 29, 30]. This Lagrangian density was initially proposed (but not solved) in Ref. [12], once its focus was in the Chern-Simons O(3) gauge sigma model. It was also addressed in Ref. [13], where the self-duality of the MCS $\sigma$ M was considered, but without developing the numerical solutions for the self-dual configurations. Here, the numerical solutions for MCS $\sigma$  M will be achieved, solved and used as a suitable background for physical comparisons.

A consistent description of the self-dual configurations carrying electric field in (1+3) dimensions also requires the introduction of the neutral scalar field appearing Lagrangian (9), being given by the following (1+3)-dimensional model:

$$\begin{aligned} \mathcal{L} = & -\frac{1}{4}F_{\alpha\beta}F^{\alpha\beta} - \frac{1}{4}\epsilon^{\alpha\beta\rho\sigma} (k_{AF})_{\alpha} A_{\beta}F_{\rho\sigma} \\ & + \frac{1}{2}D^{\alpha}\vec{\phi} \cdot D_{\alpha}\vec{\phi} + \frac{1}{2}(k_{\phi\phi})^{\alpha\beta} D_{\alpha}\vec{\phi} \cdot D_{\beta}\vec{\phi} \\ & + \frac{1}{2}\partial_{\mu}\Psi\partial^{\mu}\Psi - \frac{1}{2}[1 + (k_{\phi\phi})_{00}][(\phi_1)^2 + (\phi_2)^2]\Psi^2 \\ & - U(|\phi|, \Psi), \end{aligned} \quad (10)$$

where  $U(|\phi|, \Psi)$  is a convenient potential providing charged BPS configurations. The (1+2)-dimensional projection of the Lagrangian density (10) engenders a modified version of the MCS $\sigma$ M model (9) with the CFJ term becoming  $(k_{AF})_3 \epsilon^{\beta\rho\sigma} A_{\beta}F_{\rho\sigma}$ , and the coefficient  $(k_{AF})_3$  playing the role of the Chern-Simons mass ( $\kappa$ ). The difference rests in the presence of LV terms in the sigma sector.

### III. THE BPS FORMALISM

We are interested in finding first-order self-dual differential (BPS) equations whose solutions are minimum energy configurations that also solve the second-order Euler-Lagrange equations. To carry out the BPS procedure, we first write the stationary energy of the (1+2)-dimensional version of the model (10),

$$\begin{aligned} E = & \int d^2x \left\{ \frac{1}{2} [\delta_{ij} - (k_{\phi\phi})_{ij}] D_i\vec{\phi} \cdot D_j\vec{\phi} \right. \\ & + \frac{1}{2}B^2 + U + \frac{1}{2}(\partial_j A_0)^2 + \frac{1}{2}(\partial_j \Psi)^2 \\ & + \frac{1}{2} [1 + (k_{\phi\phi})_{00}] [(\phi_1)^2 + (\phi_2)^2] (A_0)^2 \\ & \left. + \frac{1}{2} [1 + (k_{\phi\phi})_{00}] [(\phi_1)^2 + (\phi_2)^2] \Psi^2 \right\}, \end{aligned} \quad (11)$$

which is positive definite as long as

$$\delta_{jk} - (k_{\phi\phi})_{jk} > 0, (k_{\phi\phi})_{00} > -1. \quad (12)$$

In order to implement the BPS procedure, we define  $\tilde{D}_k\vec{\phi} = M_{kj}D_j\vec{\phi}$ , which allows one to write

$$\begin{aligned} [\delta_{ij} - (k_{\phi\phi})_{ij}] D_i\vec{\phi} \cdot D_j\vec{\phi} &= \tilde{D}_k\vec{\phi} \cdot \tilde{D}_k\vec{\phi} \\ &= M_{ki}M_{kj}D_i\vec{\phi} \cdot D_j\vec{\phi}, \end{aligned} \quad (13)$$

where the  $M_{ij}$  are the elements of the matrix  $\mathbb{M}$  englobing the spatial LV parameters of the sigma sector, being defined as

$$M_{ki}M_{kj} = \delta_{ij} - (k_{\phi\phi})_{ij}. \quad (14)$$

By introducing the identity,

$$\begin{aligned} \frac{1}{2}\tilde{D}_k\vec{\phi} \cdot \tilde{D}_k\vec{\phi} &= \frac{1}{4} \left( \tilde{D}_j\vec{\phi} \pm \epsilon_{jm}\vec{\phi} \times \tilde{D}_m\vec{\phi} \right)^2 \\ &\mp (\det \mathbb{M}) \phi_3 B \pm (\det \mathbb{M}) \epsilon_{ik} \partial_i (A_k \phi_3) \\ &\pm (\det \mathbb{M}) \vec{\phi} \cdot \left( \partial_1\vec{\phi} \times \partial_2\vec{\phi} \right), \end{aligned} \quad (15)$$

the energy (11) is expressed as

$$\begin{aligned} E = & \int d^2x \left\{ \frac{1}{4} \left( \tilde{D}_j\vec{\phi} \pm \epsilon_{jm}\vec{\phi} \times \tilde{D}_m\vec{\phi} \right)^2 \right. \\ & + \frac{1}{2} \left( B \mp \sqrt{2U} \right)^2 + \frac{1}{2} (\partial_j A_0 \pm \partial_j \Psi)^2 \\ & + \frac{1}{2} [1 + (k_{\phi\phi})_{00}] [(\phi_1)^2 + (\phi_2)^2] [A_0 \pm \Psi]^2 \\ & \pm (\det \mathbb{M}) \left[ \vec{\phi} \cdot \left( \partial_1\vec{\phi} \times \partial_2\vec{\phi} \right) + \epsilon_{ik} \partial_i (A_k \phi_3) \right] \\ & \pm B\sqrt{2U} \mp (\det \mathbb{M}) \phi_3 B \mp (\partial_j \Psi) (\partial_j A_0) \\ & \left. \mp [1 + (k_{\phi\phi})_{00}] [(\phi_1)^2 + (\phi_2)^2] A_0 \Psi \right\}. \end{aligned} \quad (16)$$

Using the Gauss law (7), the last row reads as

$$\mp \Psi \partial_j \partial_j A_0 \pm (k_{AF})_3 B \Psi, \quad (17)$$

so that the energy reads

$$\begin{aligned} E = & \int d^2x \left\{ \frac{1}{4} \left( \tilde{D}_j\vec{\phi} \pm \epsilon_{jm}\vec{\phi} \times \tilde{D}_m\vec{\phi} \right)^2 \right. \\ & + \frac{1}{2} \left( B \mp \sqrt{2U} \right)^2 + \frac{1}{2} (\partial_j A_0 \pm \partial_j \Psi)^2 \\ & + \frac{1}{2} [1 + (k_{\phi\phi})_{00}] [(\phi_1)^2 + (\phi_2)^2] [A_0 \pm \Psi]^2 \\ & \pm (\det \mathbb{M}) \left[ \vec{\phi} \cdot \left( \partial_1\vec{\phi} \times \partial_2\vec{\phi} \right) + \epsilon_{ik} \partial_i (A_k \phi_3) \right] \\ & \left. \pm B \left[ \sqrt{2U} - (\det \mathbb{M}) \phi_3 + (k_{AF})_3 \Psi \right] \mp \partial_j (\Psi \partial_j A_0) \right\}. \end{aligned} \quad (18)$$

In the fifth row, one requires the factor multiplying the magnetic field to be null, which leads to the BPS potential

$$U = \frac{1}{2} [(\det \mathbb{M}) \phi_3 - (k_{AF})_3 \Psi]^2. \quad (19)$$

The integration of the expression in the fourth row of Eq. (18),

$$T_0 = \frac{(\det \mathbb{M})}{4\pi} \int d^2x \left[ \vec{\phi} \cdot \left( \partial_1 \vec{\phi} \times \partial_2 \vec{\phi} \right) + \epsilon_{ik} \partial_i (A_k \phi_3) \right], \quad (20)$$

provides the topological charge of the model, which shows dependence on the Lorentz-violating coefficients belonging to the sigma sector [30]. As it was also reported in Ref. [30], the topological conserved current is

$$K_\mu = \frac{(\det \mathbb{M})}{8\pi} \epsilon_{\mu\alpha\beta} \left[ \vec{\phi} \cdot \left( D^\alpha \vec{\phi} \times D^\beta \vec{\phi} \right) + F^{\alpha\beta} \phi_3 \right], \quad (21)$$

whose component  $K_0$ , whenever integrated over the space, yields the conserved topological charge (20). By considering the fields  $\Psi$  and  $A_0$  going to zero at infinity, in the fifth row of Eq. (18) the integration of the term  $\partial_j (\Psi \partial_j A_0)$  gives null contribution to the energy. Thus, the energy of the solutions becomes

$$\begin{aligned} E &= 4\pi T_0 \\ &+ \int d^2x \left\{ \frac{1}{2} (B \mp [(\det \mathbb{M}) \phi_3 - (k_{AF})_3 \Psi])^2 \right. \\ &+ \frac{1}{4} \left( \tilde{D}_j \vec{\phi} \pm \epsilon_{jm} \vec{\phi} \times \tilde{D}_m \vec{\phi} \right)^2 + \frac{1}{2} (\partial_j A_0 \pm \partial_j \Psi)^2 \\ &\left. + \frac{1}{2} [1 + (k_{\phi\phi})_{00}] [(\phi_1)^2 + (\phi_2)^2] [A_0 \pm \Psi]^2 \right\}. \end{aligned} \quad (22)$$

This equation allows us to establish that the energy has a lower bound given by

$$E \geq \pm 4\pi T_0, \quad (23)$$

attained whenever the fields satisfy the following self-dual or BPS equations,

$$\tilde{D}_j \vec{\phi} \pm \epsilon_{jm} \vec{\phi} \times \tilde{D}_m \vec{\phi} = 0, \quad (24)$$

$$B = \pm [(\det \mathbb{M}) \phi_3 - (k_{AF})_3 \Psi], \quad (25)$$

$$\partial_i A_0 \pm \partial_i \Psi = 0, \quad (26)$$

$$A_0 \pm \Psi = 0. \quad (27)$$

The condition  $\Psi = \mp A_0$  saturates the two last equations and the self-dual charged configurations are described by

$$\tilde{D}_j \vec{\phi} \pm \epsilon_{jm} \vec{\phi} \times \tilde{D}_m \vec{\phi} = 0, \quad (28)$$

$$B = \pm (\det \mathbb{M}) \phi_3 + (k_{AF})_3 A_0, \quad (29)$$

with the modified Gauss law

$$\partial_j \partial_j A_0 - (k_{AF})_3 B = [1 + (k_{\phi\phi})_{00}] [(\phi_1)^2 + (\phi_2)^2] A_0. \quad (30)$$

It is clear that, for null Lorentz-violating parameters, we recover the BPS equations of the gauged  $O(3)$  sigma model (1). On the other hand, if we set to be null only the Lorentz-violating parameters of the sigma sector we recuperate the self-dual equations of the Maxwell-Chern-Simons  $O(3)$  sigma model (9) with  $(k_{AF})_3 = \kappa$ . Moreover, the Gauss law (30) implies the proportionality relation,

$$Q = \frac{(k_{AF})_3}{1 + (k_{\phi\phi})_{00}} \Phi, \quad (31)$$

between the total charge ( $Q$ ) of the self-dual configurations and the total magnetic flux ( $\Phi$ ),

$$Q = - \int d^2x [(\phi_1)^2 + (\phi_2)^2] A_0, \quad (32)$$

$$\Phi = \int d^2x B. \quad (33)$$

Our analysis will also compare the Lorentz-violating solutions with the profiles of the corresponding models without Lorentz violation at all, provided by the Lagrangian densities (1) and (9). The self-dual equation for the gauge  $O(3)$  sigma model (1) are given by

$$D_j \vec{\phi} \pm \epsilon_{jm} \vec{\phi} \times D_m \vec{\phi} = 0, \quad (34)$$

$$B = \pm \phi_3, \quad (35)$$

whereas for the MCS $\sigma$ M model (9), the BPS equations and Gauss law describing self-dual configurations read as

$$D_j \vec{\phi} \pm \epsilon_{jm} \vec{\phi} \times D_m \vec{\phi} = 0, \quad (36)$$

$$B = \pm \phi_3 + \kappa A_0, \quad (37)$$

$$\partial_j \partial_j A_0 - \kappa B = [(\phi_1)^2 + (\phi_2)^2] A_0, \quad (38)$$

respectively. For this latter case, the charge and magnetic flux fulfill,  $Q = \kappa \Phi$ .

In the sequel we study the axially symmetrical self-dual solutions describing electrically charged vortices in  $CPT$ -odd Lorentz-violating framework, comparing them with solutions of the usual models preserving Lorentz invariance.

#### IV. AXIALLY SYMMETRICAL SELF-DUAL CHARGED VORTICES

For the energy to be finite, the field  $\vec{\phi}$  should go asymptotically to one of the minimum configurations of the potential, stated in Eq. (19). This is reached following

the *Ansatz* introduced in Ref. [30] for axially symmetric vortices in the presence of Lorentz violation,

$$\begin{aligned}\phi_1 &= \sin g(r) \cos\left(\frac{n}{\Lambda}\theta\right), \quad \phi_2 = \sin g(r) \sin\left(\frac{n}{\Lambda}\theta\right), \\ \phi_3 &= \cos g(r), \quad A_\theta = -\frac{1}{r}\left[a(r) - \frac{n}{\Lambda}\right], \quad A_0 = A_0(r),\end{aligned}\quad (39)$$

with the radial functions,  $g(r)$ ,  $a(r)$  and  $A_0(r)$  being well behaved and satisfying the following boundary conditions (see Sec. IV A):

$$\begin{aligned}g(0) &= 0, \quad a(0) = \frac{n}{\Lambda}, \quad A'_0(0) = 0, \\ g(\infty) &= \frac{\pi}{2}, \quad a(\infty) = 0, \quad A_0(\infty) = 0,\end{aligned}\quad (40)$$

which are compatible with the vacuum configurations of the potential for  $r \rightarrow \infty$ , while providing consistent solutions at  $r = 0$ . The non-null integer  $n$  is the winding number of the self-dual vortices. The constant  $\Lambda$  is defined in terms of the Lorentz-violating parameters belonging to the sigma sector,

$$\Lambda = \sqrt{\frac{1 - (k_{\phi\phi})_{\theta\theta}}{1 - (k_{\phi\phi})_{rr}}}. \quad (41)$$

In the *Ansatz* (39), the magnetic field  $B$  reads

$$B(r) = -\frac{a'}{r}, \quad (42)$$

where ( $'$ ) stands for the radial derivative. The BPS equations (28) and (29), projected on the *Ansatz* (39), become

$$g' = \pm \Lambda \frac{a}{r} \sin g, \quad (43)$$

$$-\frac{a'}{r} = \pm \eta \cos g + (k_{AF})_3 A_0, \quad (44)$$

whereas the Gauss law (30) reads

$$A''_0 + \frac{A'_0}{r} - (k_{AF})_3 B = \eta \Lambda \Delta A_0 \sin^2 g, \quad (45)$$

with the parameters  $\Delta$  and  $\eta$  given by

$$\Delta = \frac{1 + (k_{\phi\phi})_{00}}{\eta \Lambda}, \quad (46)$$

$$\eta = \det \mathbb{M} = \sqrt{[1 - (k_{\phi\phi})_{\theta\theta}][1 - (k_{\phi\phi})_{rr}]}. \quad (47)$$

We use the BPS equations and the Gauss law to express the BPS energy density as

$$\mathcal{E}_{BPS} = B^2 + \eta \Lambda \left(\frac{a}{r} \sin g\right)^2 + \eta \Lambda \Delta (A_0 \sin g)^2 + (A'_0)^2, \quad (48)$$

which is positive definite because  $\eta, \Lambda, \Delta > 0$ .

Replacing the *Ansatz* (39) and the boundary conditions (40) in Eq. (20), the resulting topological charge is

$$T_0 = \frac{n}{2} \frac{\eta}{\Lambda}. \quad (49)$$

Moreover, under boundary conditions (40), the magnetic flux (33) and the electric charge (32) become

$$\Phi = 2\pi \frac{n}{\Lambda}, \quad (50)$$

$$Q = 2\pi \frac{(k_{AF})_3 n}{\eta \Lambda \Delta \Lambda}, \quad (51)$$

being both proportional to the winding number,  $n$ .

The topological charge (49) and the magnetic flux (50) differ from the Lorentz symmetric ones,  $T_0 = n/2$  and  $\Phi = 2\pi n$ , by the LV factors  $\eta, \Lambda$ . The self-dual vortices of the Lorentz-symmetric MCS $\sigma$ M model are described by

$$g' = \pm \frac{a}{r} \sin g, \quad (52)$$

$$-\frac{a'}{r} = \pm \cos g + \kappa A_0, \quad (53)$$

$$A''_0 + \frac{A'_0}{r} - \kappa B = A_0 \sin^2 g, \quad (54)$$

while the correspondent BPS energy density is

$$\mathcal{E}_{BPS} = B^2 + \left(\frac{a}{r} \sin g\right)^2 + (A_0 \sin g)^2 + (A'_0)^2. \quad (55)$$

We also write self-dual the equations for the neutral vortices of the Lorentz-symmetric gauged  $O(3)$  sigma model,

$$g' = \pm \frac{a}{r} \sin g, \quad (56)$$

$$-\frac{a'}{r} = \pm \cos g, \quad (57)$$

whose BPS energy density is

$$\mathcal{E}_{BPS} = B^2 + \left(\frac{a}{r} \sin g\right)^2. \quad (58)$$

### A. Behavior of the profiles at boundaries

We study the behavior of the solutions at boundaries by solving the BPS equations and the Gauss law (45) at the limits  $r \rightarrow 0$  and  $r \rightarrow \infty$ . Close to the origin, we obtain the following expansions

$$g(r) \approx G_n r^n + \dots, \quad (59)$$

$$a(r) \approx \frac{n}{\Lambda} - \frac{[ev^2 + (k_{AF})_3 A_0(0)]}{2} er^2 + \dots, \quad (60)$$

$$A_0(r) \approx A_0(0) + \frac{[ev^2 + (k_{AF})_3 A_0(0)]}{4} (k_{AF})_3 r^2 + \dots \quad (61)$$

We observe that Eq. (60) justifies the use of the modified *Ansatz* (40) and the boundary condition for  $a(0)$ . The constant  $A_0(0)$  in (61) is determined numerically for

every  $n$ . Moreover, from (61) it is clear that the electric field must be null at origin, i.e.,  $A'(0) = 0$ , as stated in Eq. (40).

At  $r \rightarrow \infty$ , the profiles present the following asymptotic behavior:

$$g(r) \approx \frac{\pi}{2} - C_\infty \frac{e^{-mr}}{\sqrt{r}} + \dots, \quad (62)$$

$$a(r) \approx \frac{mC_\infty}{\Lambda} \sqrt{r} e^{-mr} + \dots, \quad (63)$$

$$A_0(r) \approx \frac{C_\infty (m^2 - \eta\Lambda)}{\Lambda (k_{AF})_3} \frac{e^{-mr}}{\sqrt{r}} + \dots, \quad (64)$$

where  $C_\infty$  is a positive constant determined numerically. Thus, the profiles behave in a similar way to the vortices of Abrikosov-Nielsen-Olesen [34]. The parameter  $m$  is real and positive,

$$m = \frac{1}{2} \sqrt{(k_{AF})_3^2 + \eta\Lambda (1 + \sqrt{\Delta})^2} - \frac{1}{2} \sqrt{(k_{AF})_3^2 + \eta\Lambda (1 - \sqrt{\Delta})^2}, \quad (65)$$

which is associated to the mass of the self-dual bosons and to the extension of the defect.

Now we analyze the behavior of the profiles by studying some values of the Lorentz-violating parameters involved in the bosonic mass. For fixed  $(k_{AF})_3$ , the behavior of the vortex profiles is governed by the LV coefficients belonging only to the sigma sector. In this scenario we can analyze two situations of interest: the first one occurs when  $\Delta = 1$ , providing

$$m = \frac{1}{2} \sqrt{(k_{AF})_3^2 + 4\eta\Lambda} - \frac{1}{2} |(k_{AF})_3|. \quad (66)$$

This is the mass the MCS $\sigma$ M [12],[13] would have in the presence of Lorentz violation only in the sigma sector. Indeed, for  $\eta = \Lambda = 1$  (absence of LV terms in the sigma sector), it becomes

$$m = \frac{1}{2} \sqrt{(k_{AF})_3^2 + 4} - \frac{1}{2} |(k_{AF})_3|, \quad (67)$$

the same mass of the Maxwell-Chern-Simons  $O(3)$  sigma model [13].

The second regime to be highlighted happens when  $\Delta$  takes sufficiently large values [ $\Delta \gg (k_{AF})_3$ ]:

$$m \rightarrow \sqrt{\eta\Lambda}, \quad (68)$$

corresponding to the bosonic mass of the gauged  $O(3)$  sigma model of Ref. [30] with Lorentz violation in the sigma sector (only).

Another interesting limit occurs by fixing the Lorentz-violating parameters of the sigma sector and considering sufficiently large values of  $(k_{AF})_3$ , that is

$$m \rightarrow \frac{\eta\Lambda\sqrt{\Delta}}{(k_{AF})_3}, \quad (69)$$

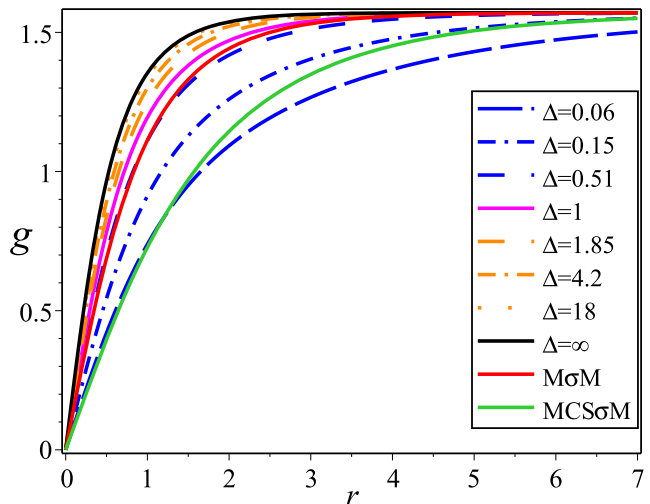


FIG. 1: Sigma field  $g(r)$  profiles.

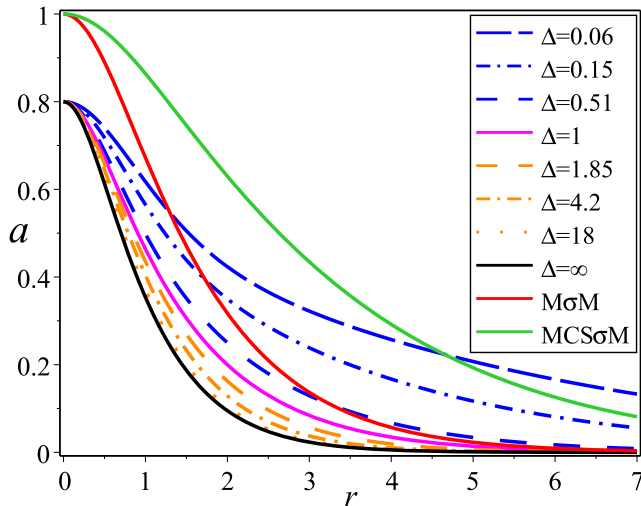
which corresponds to the mass the self-dual vortices of the Chern-Simons  $O(3)$  sigma model of Ref. [9],[12] would possess considering Lorentz violation only in the sigma sector. In this limit, taking  $(k_{\phi\phi})_{\mu\nu} = 0$  or  $\eta = \Lambda = \Delta = 1$  leads to the Lorentz symmetric mass  $(1/(k_{AF})_3)$ .

## B. Numerical analysis

Below, we depict the profiles obtained from numerical solutions of Eqs. (43)-(45), under boundary conditions (40), for winding number  $n = 1$ . We have fixed the Lorentz violating parameters  $\Lambda = 1.25$ ,  $\eta = 2$  and  $(k_{AF})_3 = 1.5$ , allowing the parameter  $\Delta$  to be free. Because the BPS energy density (48) is positive definite for  $\Delta > 0$ , we consider two regions:  $0 < \Delta < 1$  (blue lines) and  $\Delta > 1$  (orange lines), in which the behavior of the solutions are different.

There are two interesting values or limits of  $\Delta$  that allow one to recover the behavior of two known models in the presence of LV coefficients. The first one is  $\Delta = 1$  (solid magenta line), whose profiles correspond to Maxwell-Chern-Simons  $O(3)$  sigma model with Lorentz violation only in the sigma sector [see comment after Eq. (66)]. The second one is the limit  $\Delta \rightarrow \infty$  (solid black line), yielding the gauged  $O(3)$  sigma model with Lorentz violation only in the sigma sector [30] [see comment after Eq. (68)]. We also have depicted the symmetric profiles corresponding to: (i) the Maxwell-Chern-Simons gauged  $O(3)$  sigma model (9) (green solid lines) with  $\kappa = (k_{AF})_3 = 1.5$  and  $(k_{\phi\phi})_{\mu\nu} = 0$ , (ii) the gauged  $O(3)$  sigma model (1) (red solid lines) which corresponds to the total absence of Lorentz-violation [ $(k_{AF})_\mu = 0$ ,  $(k_{\phi\phi})_{\mu\nu} = 0$ ]. These two cases will serve as comparison basis to the Lorentz-violating profiles.

Figure 1 depicts the profiles of the sigma field. For

FIG. 2: Vector potential  $a(r)$  profiles.

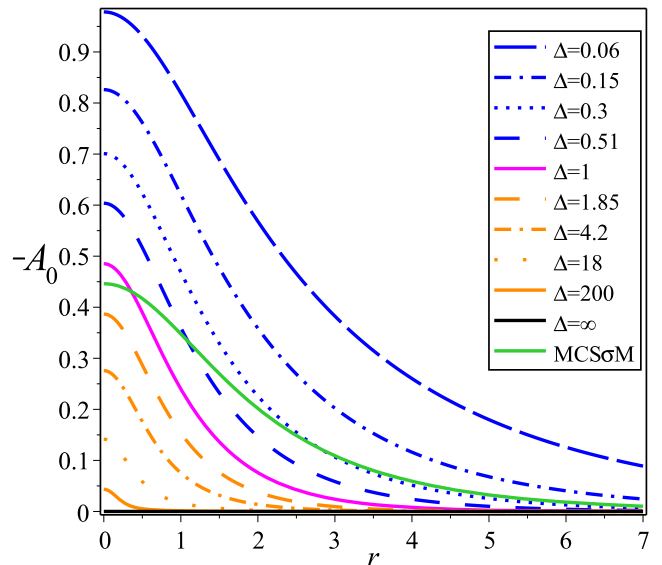
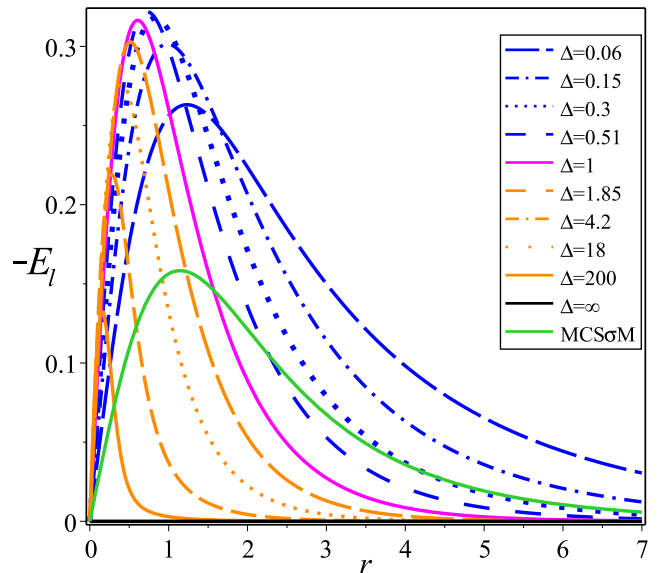
$0 < \Delta < 1$ , the profiles are more spread and saturate the asymptotic value  $\pi/2$  more slowly when  $\Delta \rightarrow 0$  (blue lines). On the other hand, for  $\Delta > 1$ , the profiles are progressively narrower for growing  $\Delta$  (orange lines), the maximum tightness being achieved in the limit  $\Delta \rightarrow \infty$  (solid black line). Thus, the profiles for  $\Delta > 1$  are confined between the models described by  $\Delta = 1$  and  $\Delta \rightarrow \infty$ .

A similar description can be given for the profiles of the vector field  $a(r)$ , presented in Fig. 2. It is worthwhile to note that the gauge field value at the origin changes from  $a(0) = n$  (in the absence of LV) to  $a(0) = n/\Delta$  (in the presence of LV in the sigma sector), which is evident in this graphic.

Figure 3 depicts the profiles for the scalar potential. For  $0 < \Delta < 1$  (blue lines), the profiles are more extended and with greater intensity at the origin. The influence of the CFJ parameter,  $(k_{AF})_3$ , is more pronounced when  $\Delta \rightarrow 0$ , while for  $\Delta > 1$  (orange lines) its effect becomes negligible for increasing values of  $\Delta$ . So, for large values of  $\Delta$  the profiles become smaller and smaller, overlapping the horizontal axis in the limit  $\Delta \rightarrow \infty$  (solid black line). It means that the vortices become electrically neutral such as the ones of the usual Lorentz-invariant gauged  $O(3)$  sigma model, in this limit.

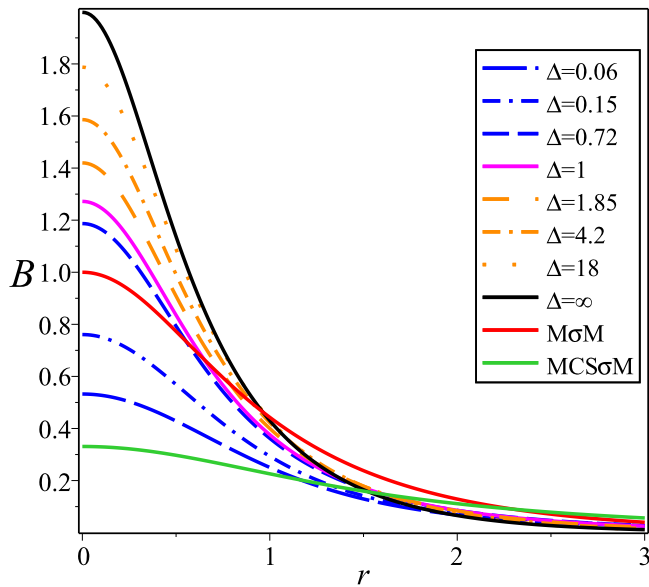
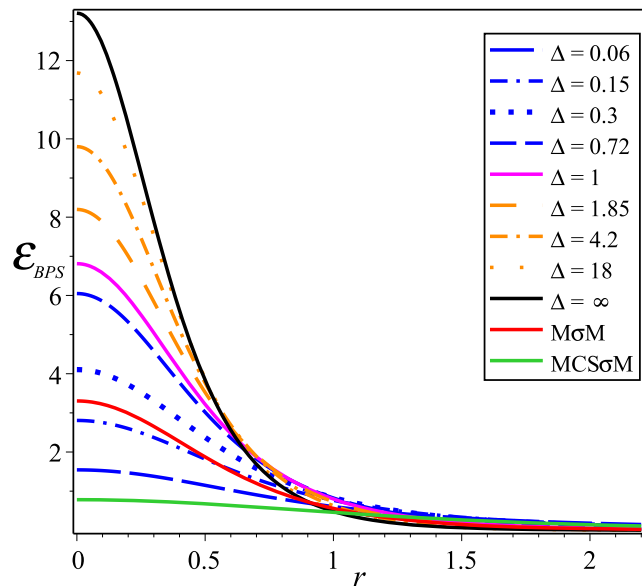
Figure 4 describes the behavior for the electric field. For  $n = 1$ , the maximum electric field amplitude is reached for some value  $\Delta^*$  such that  $0.5 < \Delta^* < 1$ . For  $0 < \Delta < 1$ , the profiles become radially more spread out for decreasing  $\Delta$  values, i.e.,  $\Delta \rightarrow 0$ . On the other hand, for  $\Delta > 1$ , the profiles are located closer to the origin, being narrower, with their amplitude decaying rapidly for increasing values of  $\Delta$ . In the limit  $\Delta \rightarrow \infty$ , the electric field disappears, which agrees with electrically uncharged vortices.

Figure 5 shows the profiles for the magnetic field, which are lumps centered at the origin for  $n = 1$ . For  $0 < \Delta < 1$  (blue lines), the profiles are more spread out and their

FIG. 3: Scalar potential  $A_0(r)$  profiles.FIG. 4: Electric field  $E_l(r) = -A'_0(r)$  profiles.

amplitude at the origin decreases continuously when  $\Delta$  goes to zero. For  $\Delta > 1$  (orange lines), the profiles become narrower and attain higher amplitudes for progressively increasing  $\Delta$ . Nevertheless, the maximum narrowness and amplitude are reached in the limit  $\Delta \rightarrow \infty$  (solid black line). Similarly, as it occurs with the sigma and vector fields, the magnetic field profiles are located between the models defined by  $\Delta = 1$  and  $\Delta \rightarrow \infty$ . The magnetic field at the origin,  $B(0)$  can be increased or reduced in relation to the Lorentz symmetric case.

For  $n = 1$ , the profiles of the BPS energy density (see Fig. 6) are lumps centered at the origin, such as the ones of the magnetic field. For increasing values of  $\Delta$ , the am-

FIG. 5: Magnetic field  $B(r)$  profiles.FIG. 6: Energy density  $\varepsilon_{BPS}(r)$  profiles.

plitude grows at the origin, the vortex core becomes more localized than the one of the Lorentz symmetric counterpart (solid green or red lines). Similarly to the magnetic field case, the maximum amplitude and narrowness occur in the limit  $\Delta \rightarrow \infty$ .

By analyzing the profiles of the magnetic field and BPS energy density for  $n > 1$  and  $\Delta$  finite, when the rotational symmetry is considered, a ringlike profile is set out, whose values at origin and maximum amplitude increase with  $\Delta$ . The ringlike structure of the magnetic field mimics the behavior of the ones in models endowed with the Chern-Simons term in the gauge sector, modifying the value and behavior at and near the origin, however.

## V. REMARKS AND CONCLUSIONS

We have developed a comprehensive study about the electrically charged self-dual configurations of the gauged  $O(3)$  nonlinear sigma model supplemented with a  $CPT$ -odd LV term in the gauge sector and a  $CPT$ -even LV term in the sigma sector. We have verified that, for supporting charged BPS solutions, the original model must be modified by introducing a neutral scalar field with appropriate dynamics, in the same manner as it happens with the Maxwell-Chern-Simons-Higgs model or the Maxwell-Chern-Simons  $O(3)$  sigma model. We have managed to implement the Bogomol'nyi-Prasad-Sommerfield formalism, finding the first order differential equations describing self-dual charged configurations whose total energy is proportional to the topological charge of the model, which gains LV contributions belonging to the sigma sector. We have also observed that the total electric charge and the total magnetic flux are related to each other such as it is shown in Eq. (31). These charged BPS configurations can be considered as classical solutions related to an extended supersymmetric theory [35] in a Lorentz-violating framework.

In particular, we have made an analysis of the axially symmetric vortex solutions of the self-dual equations, demonstrating that the total BPS energy, the magnetic flux and the electric charge are quantized (proportional to the winding number) and also proportional to the LV coefficients introduced in the sigma sector. A remarkable feature is that, choosing some limits for the LV parameters, it is possible to reproduce other gauged sigma models in the presence of Lorentz violation, like the Maxwell-Chern-Simons  $O(3)$  sigma model ( $\Delta = 1$ ) and the gauged  $O(3)$  sigma model ( $\Delta \rightarrow \infty$ ) or Chern-Simons  $O(3)$  sigma model [for very large values of  $(k_{AF})_3$ ], all them modified by Lorentz violation only in the sigma sector. In general, Lorentz violation engenders altered solutions in relation to the MCS $\sigma$ M or M $\sigma$ M profiles, as explicitly depicted in Figs. 1–6. More specifically, LV affects the behavior of the magnetic field and BPS energy density at the origin and near the origin: the amplitude augments with  $\Delta$ , reaching its maximum deviation in the limit  $\Delta \rightarrow \infty$ , while the width decreases, yielding more compact and localized vortex profiles (for large values of  $\Delta$ ). Thus, the LV defects have amplitude more pronounced near the origin and are much more localized than the Lorentz invariant solutions. An investigation to be yet done concerns the influence of Lorentz symmetry violation on the dynamics of these types of vortices.

## Acknowledgments

R. C. and M. M. F. J. thank CNPq and FAPEMA (Brazilian agencies) for financial support. C. F. F. and G. L. thank CAPES (Brazilian agency) for full financial support



- 
- [1] M. Gell-Mann and M. Levy, *Nuovo Cimento* **16**, 705 (1960)
- [2] J. Schwinger, *Ann. Phys. (N.Y.)* **2**, 407 (1957).
- [3] J. C. Polkinghorne *Nuovo Cimento* **8**, 179 (1958); **8**, 781 (1958).
- [4] A. A. Belavin and A. M. Polyakov, *JETP Lett.* **22**, 245 (1975).
- [5] R. Rajaraman, *Solitons and Instantons*, (North-Holland, Amsterdam, 1982); W. J. Zakrzewski, *Low Dimensional Sigma Models* (Hilger, Bristol, 1989).
- [6] E. B. Bogomol'nyi, *Sov. J. Nucl. Phys.* **24**, 449 (1976); M. Prasad and C. Sommerfield, *Phys. Rev. Lett.* **35**, 760 (1975).
- [7] R. A. Leese, M. Peyrard, and W. J. Zakrzewski, *Nonlinearity* **3**, 387 (1990).
- [8] B. J. Schroers, *Phys. Lett. B* **356**, 291 (1995).
- [9] P. K. Ghosh and S. K. Ghosh, *Phys. Lett. B* **366**, 199 (1996).
- [10] P. Mukherjee, *Phys. Lett. B* **403**, 70 (1997).
- [11] P. Mukherjee, *Phys. Rev. D* **58**, 105025 (1998).
- [12] K. Kimm, K. Lee, and T. Lee, *Phys. Rev. D* **53**, 4436 (1996).
- [13] J. Han and H.-S. Nam, *Lett. Math. Phys.* **73**, 17 (2005).
- [14] F. S. A. Cavalcante, M.S. Cunha, and C.A.S. Almeida, *Phys. Lett. B* **475**, 315 (2000); M. S. Cunha, R. R. Landim, and C. A. S. Almeida, *Phys. Rev. D* **74**, 067701 (2006).
- [15] D. Colladay and V. A. Kostelecky, *Phys. Rev. D* **55**, 6760 (1997); **58**, 116002 (1998).
- [16] S. R. Coleman and S. L. Glashow, *Phys. Rev. D* **59**, 116008 (1999).
- [17] F. R. Klinkhamer and M. Schreck, *Nucl. Phys. B* **848**, 90 (2011); M. Schreck, *Phys. Rev. D* **86**, 065038 (2012); M.A. Hohensee, R. Lehnert, D. F. Phillips, and R. L. Walsworth, *Phys. Rev. D* **80**, 036010 (2009); A. Moyotl, H. Novales-Sánchez, J. J. Toscano, and E. S. Tututi, *Int. J. Mod. Phys. A* **29**, 1450039 (2014); **29**, 1450107 (2014); M. Cambiaso, R. Lehnert, and R. Potting, *Phys. Rev. D* **90**, 065003 (2014); R. Bufalo, *Int. J. Mod. Phys. A* **29**, 1450112 (2014); C.M. Reyes, L. F. Urrutia, and J. D. Vergara, *Phys. Rev. D* **78**, 125011 (2008); *Phys. Lett. B* **675**, 336 (2009); C. M. Reyes, *Phys. Rev. D* **82**, 125036 (2010); **80**, 105008 (2009); **87**, 125028 (2013).
- [18] V. A. Kostelecky and C. D. Lane, *J. Math. Phys. (N.Y.)* **40**, 6245 (1999); R. Lehnert, *J. Math. Phys. (N.Y.)* **45**, 3399 (2004); D. Colladay and V. A. Kostelecky, *Phys. Lett. B* **511**, 209 (2001); V. A. Kostelecky, C. D. Lane, and A. G. M. Pickering, *Phys. Rev. D* **65**, 056006 (2002); C. D. Carone, M. Sher, and M. Vanderhaeghen, *Phys. Rev. D* **74**, 077901 (2006); W.F. Chen and G. Kunstatter, *Phys. Rev. D* **62**, 105029 (2000); O. M. Del Cima, D. H. T. Franco, A. H. Gomes, J. M. Fonseca, and O. Piguet, *Phys. Rev. D* **85**, 065023 (2012); T. R. S. Santos and R. F. Sobreiro, *Phys. Rev. D* **91**, 025008 (2015).
- [19] M. A. Anacleto, F. A. Brito, and E. Passos, *Phys. Rev. D* **86**, 125015 (2012); M. A. Anacleto, *Phys. Rev. D* **92**, 085035 (2015); E. O. Silva and F. M. Andrade, *Europhys. Lett.* **101**, 51005 (2013); F.M. Andrade, E. O. Silva, T. Prudêncio, and C. Filgueiras, *J. Phys. G* **40** 075007 (2013).
- [20] M. N. Barreto, D. Bazeia, and R. Menezes, *Phys. Rev. D* **73**, 065015 (2006); A. de Souza Dutra, M. Hott, and F. A. Barone, *Phys. Rev. D* **74**, 085030 (2006); A. de Souza Dutra and R. A. C. Correa, *Phys. Rev. D* **83**, 105007 (2011); R. A. C. Correa, R. da Rocha, and A. de Souza Dutra, *Ann. Phys. (Amsterdam)* **359**, 198 (2015).
- [21] M.D. Seifert, *Phys. Rev. Lett.* **105**, 201601 (2010); *Phys. Rev. D* **82**, 125015 (2010).
- [22] N.M. Barraz Jr., J.M. Fonseca, W.A. Moura-Melo, and J. A. Helayel-Neto, *Phys. Rev. D* **76**, 027701 (2007); A. P. Baeta Scarpelli and J. A. Helayel-Neto, *Phys. Rev. D* **73**, 105020 (2006).
- [23] A. de Souza Dutra and R. A. C. Correa, *Adv. High Energy Phys.* **2015**, 673716 (2015); R. A. C. Correa, R. da Rocha, and A. de Souza Dutra, *Phys. Rev. D* **91**, 125021 (2015).
- [24] C. Miller, R. Casana, M. M. Ferreira Jr., and E. da Hora, *Phys. Rev. D* **86**, 065011 (2012).
- [25] R. Casana, M. Ferreira Jr., E. da Hora, and C. Miller, *Phys. Lett. B* **718**, 620 (2012).
- [26] L. Sourrouille, *Phys. Rev. D* **89**, 087702 (2014); R. Casana and L. Sourrouille, *Phys. Lett. B* **726**, 488 (2013).
- [27] C.H. Coronado Villalobos, J.M. Hoff da Silva, M.B. Hott, and H. Belich, *Eur. Phys. J. C* **74**, 27991 (2014).
- [28] H. Belich, F.J.L. Leal, H.L.C. Louzada, and M.T.D. Orlando, *Phys. Rev. D* **86**, 125037 (2012).
- [29] R. Casana and G. Lazar, *Phys. Rev. D* **90**, 065007 (2014).
- [30] R. Casana, C. F. Farias, and M. M. Ferreira Jr., *Phys. Rev. D* **92**, 125024 (2015).
- [31] S. M. Carroll, G.B. Field, and R. Jackiw, *Phys. Rev. D* **41**, 1231 (1990).
- [32] C. K. Lee, K.M. Lee, and H. Min, *Phys. Lett. B* **252**, 79 (1990).
- [33] S. Bolognesi and S.B. Gudnason, *Nucl. Phys. B* **805**, 104 (2008).
- [34] A. A. Abrikosov, *Zh. Eksp. Teor. Fiz.* **32**, 1442 (1957) [*Sov. Phys. JETP* **5**, 1174 (1957)]; H. Nielsen and P. Olesen, *Nucl. Phys.* **B61**, 45 (1973).
- [35] E. Witten and D. Olive, *Phys. Lett. B* **78**, 97 (1978).